



Evaluating the added value of synthetic magnetic resonance imaging in predicting sentinel lymph node status in breast cancer

Xiao Yang¹, Zhou Lu¹, Xiaoying Tan¹, Lin Shao¹, Jie Shi², Weiqiang Dou², Zongqiong Sun¹

¹Department of Radiology, Affiliated Hospital of Jiangnan University, Wuxi, China; ²GE Healthcare, MR Research China, Beijing, China

Contributions: (I) Conception and design: X Yang, Z Sun; (II) Administrative support: J Shi, W Dou; (III) Provision of study materials or patients: X Yang, Z Lu; (IV) Collection and assembly of data: X Tan, L Shao; (V) Data analysis and interpretation: J Shi, W Dou; (VI) Manuscript writing: All authors; (VII) Final approval of manuscript: All authors.

Correspondence to: Zongqiong Sun, MD. Department of Radiology, Affiliated Hospital of Jiangnan University, Hefeng Road 1000#, Binhu District, Wuxi, China. Email: qiong953780@163.com.

Background: The noninvasive prediction of sentinel lymph node (SLN) metastasis using quantitative magnetic resonance imaging (MRI), particularly with synthetic MRI (syMRI), is an emerging field. This study aimed to explore the potential added benefits of syMRI over conventional MRI and diffusion-weighted imaging (DWI) in predicting metastases in SLNs.

Methods: This retrospective study consecutively enrolled 101 patients who were diagnosed with breast cancer (BC) and underwent SLN biopsy from December 2022 to October 2023 at the Affiliated Hospital of Jiangnan University. These patients underwent preoperative MRI including conventional MRI, DWI, and syMRI and were categorized into two groups according to the postoperative pathological results: those with and without metastatic SLNs. MRI morphological features, DWI, and syMRI-derived quantitative parameters of breast tumors were statistically compared between these two groups. Binary logistic regression was used to separately develop predictive models for determining the presence of SLN involvement, with variables that exhibited significant differences being incorporated. The performance of each model was evaluated through receiver operating characteristic (ROC) curve analysis, including the area under the curve (AUC), sensitivity, and specificity.

Results: Compared to the group of 54 patients with BC but no metastatic SLNs, the group of 47 patients with BC and metastatic SLNs had a significantly larger maximum axis diameter [metastatic SLNs: median 2.40 cm, interquartile range (IQR) 1.50–3.00 cm; no metastatic SLNs: median 1.80 cm, IQR 1.37–2.50 cm; $P=0.03$], a higher proton density (PD) (78.44 ± 11.92 vs. 69.20 ± 10.63 pu; $P<0.001$), and a lower apparent diffusion coefficient (ADC) (metastatic SLNs: median 0.91×10^{-3} mm²/s, IQR 0.79–1.01 mm²/s; no metastatic SLNs: median 1.02×10^{-3} mm²/s, IQR 0.92–1.12 mm²/s; $P=0.001$). Moreover, the prediction model with maximum axis diameter and ADC yielded an AUC of 0.71 [95% confidence interval (CI): 0.618–0.802], with a sensitivity of 78.72% and a specificity of 51.85%; After addition of syMRI-derived PD to the prediction model, the AUC increased significantly to 0.86 (AUC: 0.86 vs. 0.71; 95% CI: 0.778–0.922; $P=0.002$), with a sensitivity of 80.85% and a specificity of 81.50%.

Conclusions: Combined with conventional MRI and DWI, syMRI can offer additional value in enhancing the predictive performance of determining SLN status before surgery in patients with BC.

Keywords: Synthetic magnetic resonance imaging (syMRI); sentinel lymph node (SLN); metastasis; diffusion-weighted imaging (DWI); breast cancer (BC)

Submitted Jan 01, 2024. Accepted for publication Mar 29, 2024. Published online Apr 29, 2024.

doi: 10.21037/qims-24-1

View this article at: <https://dx.doi.org/10.21037/qims-24-1>

Introduction

According to the Global Cancer statistics 2020 report, breast cancer (BC) has surpassed lung cancer as the most prevalent cancer in women globally (1). Sentinel lymph node (SLN) metastasis represents the initial stage of lymph node metastasis in BC. It is a reliable indicator of axillary lymph nodes (ALN) status, particularly in patients whose ALNs are clinically negative. ALN metastases occur in fewer than 20% of early-stage breast tumors that are <1.5 cm in diameter, which has ramifications for the staging and prognosis of patients with BC (2,3). Moreover, the SLN technique is highly valuable for improving the quality of life of patients, as it can help prevent unnecessary ALN dissection, thereby reducing the length of hospitalization, the risk of infection in the axillary fossa, and the risk of lymphedema (4). Hence, determination of preoperative SLN status is crucial for accurate clinical staging and individualized treatment in patients with BC (5,6). Currently, the assessment of SLNs primarily relies on intraoperative SLN biopsy (7). However, patients are often reluctant to undergo this invasive procedure, resulting in poor compliance. Furthermore, studies have indicated that SLNs biopsy can yield false negatives, leading to inadequate treatment and the possibility of tumor recurrence or metastasis (8,9). Therefore, the development of a noninvasive imaging approach with high diagnostic efficacy would be of considerable value for the detection of SLNs.

Conventional anatomic magnetic resonance imaging (MRI), known for its excellent soft tissue resolution, has been extensively used in BC imaging (10-12). However, false-positive or false-negative results often occur due to the sole reliance on morphological features in conventional imaging models often being inadequate for revealing the internal characteristics of lesions.

Functional MRI, such as diffusion-weighted imaging (DWI) and dynamic contrast-enhanced magnetic resonance imaging (DCE-MRI), can provide quantitative information regarding the internal physiological state of BC and aid in predicting the status of SLNs (12). However, there are concerns regarding DCE-MRI related to its long scan time and the requirement of contrast agent injection. Additionally, the accurate prediction of ALN status remains challenging, as the findings reported in previous studies have been inconsistent in terms of sensitivity (67.4–86.2%) and specificity (52.4–72.1%) (10,13).

MRI compilation (MAGiC), as a vendor-provided mode of synthetic MRI (syMRI), is a relatively new quantitative imaging technique. MAGiC employs a multiecho,

multidelay acquisition technique, allowing for simultaneous quantification of the T1 and T2 relaxation times, as well as proton density (PD) images, in a matter of minutes (14-16). With these features, syMRI has demonstrated an excellent capability to distinguish between benign and malignant breast tumors and between high- and low-grade bladder and prostate cancers (17-19). Moreover, recent studies have used syMRI for the identification of lymph node status in rectal cancer and nasopharyngeal cancer (20,21). Given its promising record, we speculated that syMRI may also hold potential in predicting metastatic SLNs for patients with BC; however, to the best of our knowledge, few studies have investigated this possibility.

Therefore, the aim of this study was to investigate the feasibility of syMRI in predicting SLN metastases in BC and to further determine if syMRI enhances diagnostic efficacy when combined with conventional MRI and DWI. We present this article in accordance with the STARD reporting checklist (available at <https://qims.amegroups.com/article/view/10.21037/qims-24-1/rc>).

Methods

Study population

This study was conducted according to the Declaration of Helsinki (as revised in 2013) and was approved by the Ethics Committee of the Affiliated Hospital of Jiangnan University (No. LS2023090). The requirement for informed consent was waived due to the retrospective nature of the design. Initially, 136 consecutive patients with breast masses detected through mammography or ultrasound from December 2022 to October 2023 were included. The inclusion criteria were as follows: (I) completion of preoperative MRI scans of breast lesions, including conventional MRI, DWI, and syMRI; (II) no neoadjuvant therapy, including radiotherapy and chemotherapy, prior to breast lesion MRI scans; (III) completion of surgical resection of breast tumor and SLN biopsy within 1 week after breast MRI scans to obtain pathological results; and (IV) confirmation of BC via the pathological examination of surgically resected breast tumor. Meanwhile, the exclusion criteria were as follows: (I) breast lesions insufficiently large [maximum axial diameter (MaxAD) <5 mm] for drawing regions of interest (ROIs); (II) poor MRI image quality, with severe artifacts on DWI and/or syMRI; and (III) presence of other malignant tumors. Ultimately, 101 patients with BC, comprising 101 breast lesions, were enrolled in this study (*Figure 1*). The pathological features [histological grading,

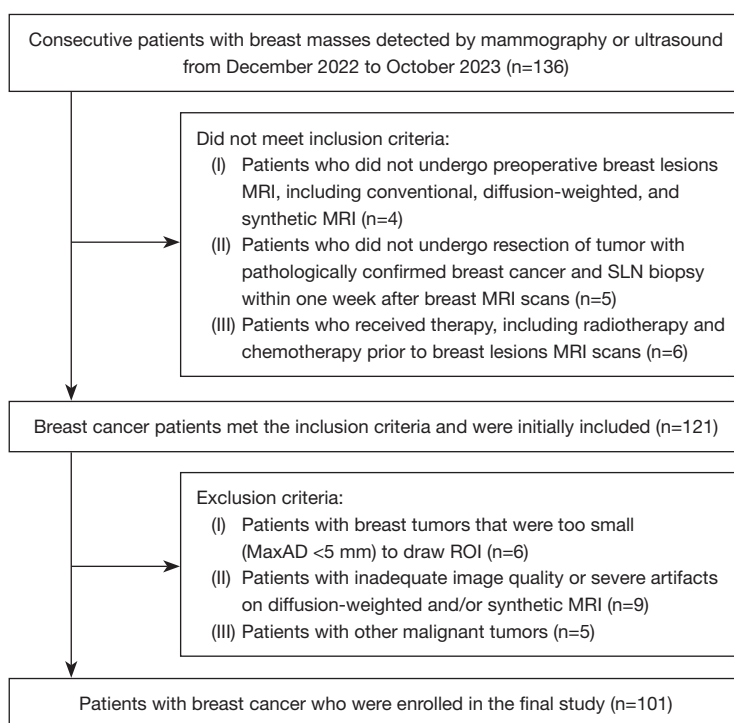


Figure 1 Flowchart of participant selection. MRI, magnetic resonance imaging; SLN, sentinel lymph node; MaxAD, maximum axis diameter; ROI, region of interest.

Ki-67 index, estrogen receptor (ER) status, progesterone receptor (PR) status, and human epidermal growth factor receptor 2 (HER2) status] of tumors were determined by immunohistochemical (IHC) examination at the department of pathology. Patients were grouped into those with and without metastatic SLNs according to the postoperative pathological results. Clinical baseline characteristics (patient age and menopausal status) of these two groups of patients were recorded from digital clinical files of the Picture Archive and Communication System (PACS).

MRI acquisition

All MRI examinations were performed on a 3.0-T scanner (Signa Architect; GE HealthCare, China) equipped with an 8-channel phased-array breast coil. All patients were positioned in a prone position, with the breasts hanging naturally in the dedicated breast coil. syMRI and DWI sequences were scanned after the routine T₁-weighted imaging (T₁WI) and T₂-weighted imaging (T₂WI) and before DCE-MRI scans. MRI sequences for T₁WI and T₂WI and the corresponding scanning parameters are detailed in Table S1. The scanning parameters for syMRI

were as follows: field of view (FOV), 36×36 cm²; repetition time (TR), 4,032 ms; echo time (TE), 24.5/97.9 ms; matrix, 320×256; echo train length, 12; number of excitations (NEX), 1; and slice thickness/gap, 4/1 mm. The acquisition time for syMRI scan was about 5 minutes.

The single-shot spin-echo echo planar imaging sequence was employed to acquire DWI, which included b values of 0 and 1,000 s/mm². The apparent diffusion coefficient (ADC) was automatically generated from DWI images. The scanning parameters for DWI were as follows: TR, 6,232 ms; TE, 76 ms; matrix, 128×132; FOV, 36×36 cm²; and slice thickness/gap, 4.0/0.4 mm. Intravenous injection of gadoteric acid (gadoteric acid meglumine injection; Jiangsu Hengrui Medicine, China) was administered at a dose of 0.2 mL/kg, with an injection rate of 2.5 mL/s. A DCE-MRI sequence was used for image acquisition, resulting in one phase of a precontrast scan followed by six phases of DE images.

Conventional MRI features of breast tumors

All breast MRI images were analyzed for conventional MRI features of breast tumors by two breast radiologists with 3

and 15 years of experience, respectively, who were blinded to pathological results of breast tumors and the status of SLNs. Based on the fifth version of the Breast Imaging Reporting and Data System (BI-RADS) (22), the evaluated features were as follows: tumor size (MaxAD), tumor shape (oval/round or irregular), T₂WI signal (hypo-/isointensity or hyperintensity), internal enhancement (homogeneous or heterogeneous), background parenchymal enhancement (minimal/mild or moderate/marked), time-intensity curve (TIC), and type of DCE-MRI (persistent, plateau, washout) (11,23). The MaxAD in the largest cross-section of each breast tumor was measured on the conventional axial T₂WI. When disagreements arose between the two radiologists, a consensus was reached through discussion.

DWI and syMRI features of breast tumors

The DWI and syMRI features of breast tumors were evaluated by the same two radiologists mentioned above. MAGiC data were postprocessed using syMRI 8.0 software (SyntheticMR) to generate quantitative T₁, T₂, and PD maps. To obtain the quantitative information of breast tumors, the ROIs were manually delineated along the tumor's edge on synthetic T₂WI, with artifacts, large vessels, necrotic areas, and cystic regions on the largest axial cross-section of breast tumor being avoided. The same ROIs were automatically prescribed on the T₁, T₂, and PD maps simultaneously. The resultant quantitative values of T₁, T₂, and PD for breast lesions were obtained. Similar tumor ROIs with the largest cross-sectional area on the ADC map were also obtained. The measured syMRI parameters (T₁, T₂, PD) and ADC were assessed for interobserver agreement between the two radiologists. The average values of the two radiologists were used for the final statistical analysis.

Histopathologic assessment

The IHC pathological results of breast tumors included the Ki-67 labeling index, ER, PR, and HER2 expression. The IHC markers were assessed based on the following criteria: If more than 1% of cell nuclei showed positive staining in 10 high-power fields, this was defined as ER or PR positive. Tumors with IHC staining scores of 0 and 1+ were considered HER2 negative. Tumors with a staining score of 2+ required further confirmation through fluorescence in situ hybridization (FISH), in which gene amplification was observed to confirm HER2 positivity.

Tumors with a staining score of 3+ were considered HER2 positive. A threshold of 14% was used to evaluate the Ki-67 expression (24). The modified Bloom-Richardson scoring system was employed to evaluate the histological grading of tumor tissue (25). Final histopathology confirmed the presence or absence of SLN metastases. As long as at least one SLN was metastatic, this was regarded as a BC case with metastatic SLNs. On the contrary, for any case of negative SLNs, this was considered a BC case without metastatic SLNs.

Statistical analysis

All statistical analyses were performed using SPSS version 25.0 (IBM Corp., USA) and MedCalc version 19.2.6 (MedCalc Software). The intergroup correlation coefficients (ICCs) and weighted kappa values were used to measure the interobserver agreement between two radiologists for the conventional features, DWI, and syMRI-derived parameters of tumors. A kappa or ICC value greater than 0.75 indicated excellent consistency. All normally or nonnormally distributed quantitative data are respectively presented as the mean \pm standard deviation or median with interquartile range (IQR), while qualitative data are presented as percentages. Quantitative parameters were compared between patients with BC with metastatic SLNs and without metastatic SLNs using either the Mann-Whitney test or Student's *t*-test based on the distribution of data and homogeneity of variances, while categorical data were compared using the Chi-square test. Univariable and multivariable logistic regression analyses (forward stepwise, logistic regression; probability for stepwise entry, 0.05; removal, 0.1) were performed to identify the independent predictive factors. The Pearson correlation coefficient was used to evaluate the correlation between quantitative parameters PD, and ADC values. The diagnostic performance of quantitative parameters and anatomic features of breast lesions in predicting metastatic SLNs was assessed using the receiver operating characteristic (ROC) curve and the area under the curve (AUC). The diagnostic cutoff value was determined using the maximum Youden index (sensitivity + specificity - 1). Joint diagnostic models based on syMRI, DWI, morphologic features were constructed to predict the probability of metastatic SLNs in BC via logistic regression. The differences between AUCs were compared using the DeLong test. If the *P* value obtained from a two-sided test was less than 0.05, the difference was considered statistically significant.

Table 1 Comparisons of the clinicopathologic characteristics between patients with breast cancer and metastatic SLNs (n=47) and those without metastatic SLNs (n=54)

Clinicopathologic characteristic	Without metastatic SLNs (n=54)	With metastatic SLNs (n=47)	P value
Age (years)	51.19±11.74	53.57±10.95	0.29
Menopausal status			0.04*
Postmenopausal	35 (64.8)	21 (44.7)	
Premenopausal	19 (35.2)	26 (55.3)	
Histological grade			0.35
1 or 2	38 (70.4)	29 (61.7)	
3	16 (29.6)	18 (38.3)	
ER status			0.11
Positive	39 (72.2)	40 (85.1)	
Negative	15 (27.8)	7 (14.9)	
PR			0.26
Positive	31 (57.4)	32 (68.1)	
Negative	23 (42.6)	15 (31.9)	
HER2			0.29
Positive	19 (35.2)	12 (25.5)	
Negative	35 (64.8)	35 (74.5)	
Ki-67			0.01*
≥14%	37 (68.5)	42 (89.4)	
<14%	17 (31.5)	5 (10.6)	

The data are the number of participants and percentages in parentheses. The values are presented as the mean ± standard deviation. *, statistical difference. SLN, sentinel lymph node; ER, estrogen receptor; PR, progesterone receptor; HER2, human epidermal growth factor receptor 2.

Results

Clinicopathological characteristics

This study ultimately recruited 101 patients with BC comprising 101 breast lesions. Among these, 84 were invasive ductal carcinoma (IDC), 11 were ductal carcinoma *in situ*, 2 were invasive lobular carcinoma, and 4 were mucinous carcinoma. All participants were females, with an average age of 52±11 years. Based on the pathological results of SLNs, 54 participants were classified as the group without metastatic SLNs, while 47 were categorized as the group with metastatic SLNs. Breast tumors with metastatic SLNs exhibited a significantly higher Ki-67 index compared to those without metastatic SLNs (P=0.01). Menopausal status was statistically different between the two groups

of patients with BC (P=0.04). No statistically significant differences were observed in clinicopathological features, including age, histological grade, ER status, PR status, and HER-2 status, between the two groups of patients with BC (Table 1).

Conventional MRI features of breast tumors

Interobserver agreements for assessing conventional MRI features of tumors were all excellent, with kappa values >0.80. Breast lesions revealed significantly statistical differences in conventional morphological features (MaxAD) between the two groups of patients with BC (P=0.03). The finding indicated that larger-sized breast tumors were more likely to result in metastatic SLNs. However, there were no statistically significant differences

Table 2 Comparisons of conventional MRI, DWI, and syMRI characteristics of breast tumors between patients with breast cancer and metastatic SLNs (n=47) and those without metastatic SLNs (n=54)

MRI features and parameters	Without metastatic SLNs (n=54)	With metastatic SLNs (n=47)	P value
MaxAD (cm)	1.80 (1.37, 2.50)	2.40 (1.50, 3.00)	0.03*
Shape			0.52
Round/oval	12 (22.2)	13 (27.7)	
Irregular	42 (77.8)	34 (72.3)	
T ₂ WI signal intensity			0.33
Hypo-/isointensity	27 (50.0)	19 (40.4)	
Hyperintensity	27 (50.0)	28 (59.6)	
Internal enhancement			0.47
Homogeneous	11 (20.4)	7 (14.9)	
Heterogeneous	43 (79.6)	40 (85.1)	
BPE			0.26
Minimal/mild	41 (75.9)	31 (66.0)	
Moderate/marked	13 (24.1)	16 (34.0)	
TIC type			0.21
Persistent	5 (9.3)	2 (4.3)	
Plateau	20 (37.0)	12 (25.5)	
Washout	29 (53.7)	33 (70.2)	
T1 (ms)	1,498.46±432.14	1,580.57±355.97	0.18
T2 (ms)	73.00 (65.50, 77.25)	72.00 (67.00, 79.00)	0.61
PD (pu)	69.20±10.63	78.44±11.92	<0.001*
ADC (×10 ⁻³ mm ² /s)	1.02 (0.92, 1.12)	0.91 (0.79, 1.01)	0.001*

The data are expressed the number of participants and percentages in parentheses. The values are presented as the median (upper quartile, lower quartile) or mean ± standard deviation. *, statistical difference. MRI, magnetic resonance imaging; DWI, diffusion-weighted imaging; syMRI, synthetic MRI; SLN, sentinel lymph node; MaxAD, maximum axis diameter; T₂WI, T2-weighted imaging; BPE, background parenchymal enhancement; TIC, time-intensity curve; T1, longitudinal relaxation time; T2, transverse relaxation time; PD, proton density; ADC, apparent diffusion coefficient.

between the two groups in terms of tumor T₂WI signal intensity, shape, internal enhancement, background parenchymal enhancement, or TIC (all P values >0.05). *Table 2* provides a comprehensive summary comparing conventional MRI features for evaluating the presence or absence of metastatic SLNs.

syMRI and DWI quantitative parameters of breast tumors

Excellent interobserver agreement was achieved as indicated by the high ICC values (>0.80) for syMRI and

DWI parameter measurements between the two observers. Furthermore, there was no significant linear correlation between ADC and PD parameters ($r=0.157$; $P=0.11$).

Compared to those without metastatic SLNs, breast tumors with metastatic SLNs exhibited a significantly higher PD ($P<0.001$) and lower ADC values ($P=0.001$). However, there were no significant differences in T1 or T2 values between groups with and without metastatic SLNs (both P values >0.05) (*Table 2* and *Figure 2*). *Figures 3* and *4* present the MRI findings of two participants without and with metastatic SLNs, respectively.

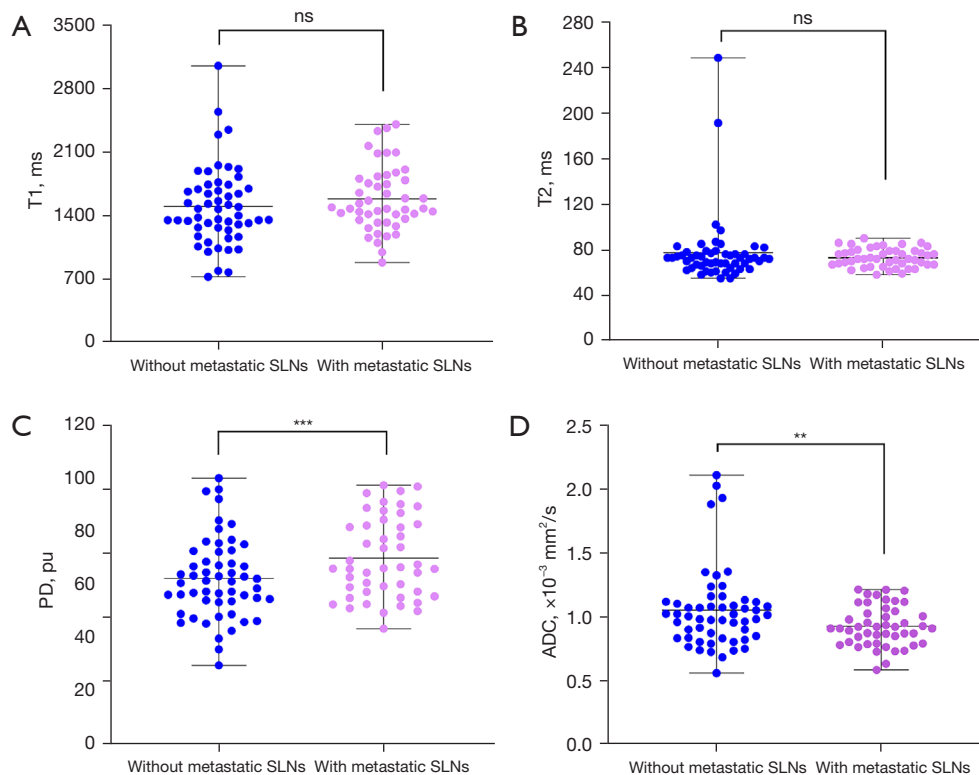


Figure 2 Scatter plot and comparisons of MRI quantitative parameters of tumors between patients with breast cancer and metastatic SLNs and those without metastatic SLNs. (A) T1, (B) T2, (C) PD, and (D) ADC. **, $P < 0.01$; ***, $P < 0.001$. ns, nonstatistical significance; SLN, sentinel lymph node; T1, T1 relaxation time; T2, T2 relaxation time; PD, proton density; ADC, apparent diffusion coefficient; MRI, magnetic resonance imaging.

The performance of MRI features and quantitative parameters of breast tumors in predicting SLNs metastases

Univariable and multivariable logistic regression analyses revealed that the morphological feature of MaxAD [odds ratio (OR): 2.162; 95% confidence interval (CI): 1.116–4.189; $P = 0.02$], the DWI parameter of ADC (OR: 0.004, 95% CI: 0.002–0.089; $P < 0.001$), and the syMRI parameter of PD (OR: 1.134; 95% CI: 1.068–1.204; $P < 0.001$) were independent predictors of metastatic SLNs in BC (Table 3).

In the ROC analyses, among all three individual variables (MaxAD, ADC, PD) with significantly statistical differences, PD demonstrated the highest diagnostic efficacy in predicting the presence or absence of metastatic SLNs in BC, with an AUC of 0.75, a sensitivity of 72.34%, and a specificity of 77.78%. The predictive joint model established from these three predictors yielded an AUC of 0.86 (95% CI: 0.778–0.922), with a sensitivity of 80.85% and a specificity of 81.50%. The combined model was superior to the MaxAD, ADC, PD, and MaxAD + ADC

according to a comparison of their AUCs (all P values < 0.01) (Table 4 and Figure 5).

Discussion

Precise preoperative assessment of SLN status in patients with BC is vital for effective clinical management and selection of appropriate surgical treatment strategies. In this study, we investigated the added value of syMRI by combining conventional morphological and diffusion-weighted MRI for predicting metastatic SLNs prior to surgery. Our results demonstrated that patients with BC and metastatic SLNs exhibited statistically higher tumor MaxAD, PD values, and lower ADC values compared to those without metastatic SLNs. Furthermore, we constructed a combined prediction model that incorporated these three tumor factors (MaxAD + ADC + PD), resulting in the highest AUC of 0.86. This finding suggests that syMRI can contribute to the prediction of metastatic

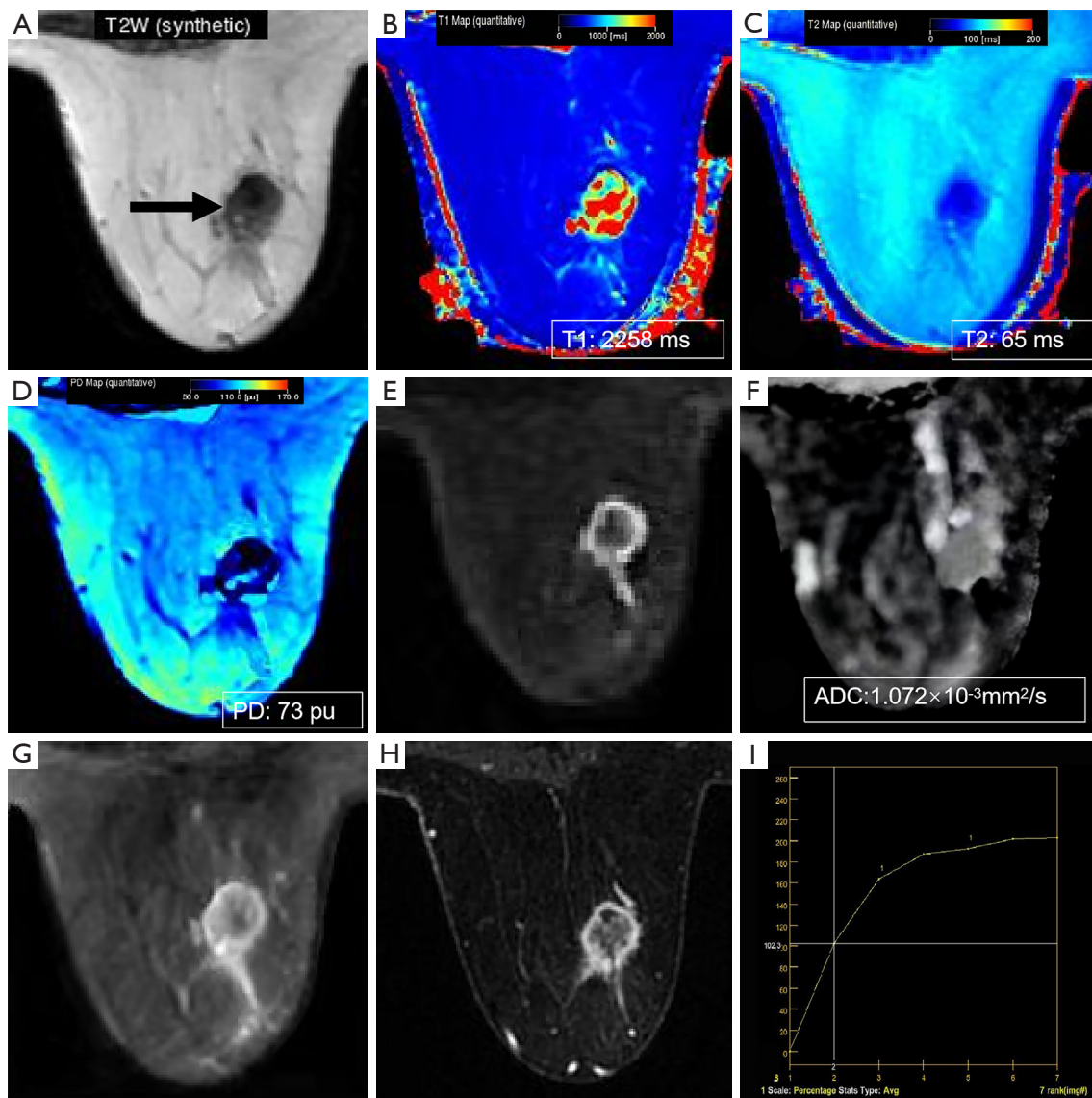


Figure 3 A 67-year-old female with breast cancer (arrow) but no metastatic SLNs. (A) Synthetic T2-weighted image. (B–D) The quantitative T1 map, T2 map, and PD map were acquired using syMRI; the T1 value of 2,258 ms, T2 value of 65 ms, and PD value of 73 pu are shown, respectively. (E) DWI ($b=1,000 \text{ s/mm}^2$) presenting inhomogenous hyperintensity in the tumor. (F) ADC map showing the ADC value of the tumor. (G) T2WI with fat saturation suppression showing a MaxAD of 2.4 cm, hyperintensity, and an oval shape of the breast tumor. (H) Contrast-enhanced image showing internal heterogeneous enhancement in the tumor. (I) TIC of DCE-MRI showing a persistent enhancement of the tumor. T2W, T2-weighted; T1, T1 relaxation time; T2, T2 relaxation time; PD, proton density; ADC, apparent diffusion coefficient; Avg, average; SLN, sentinel lymph node; syMRI, synthetic MRI; DWI, diffusion-weighted imaging; T2WI, T2-weighted imaging; MaxAD, maximum axis diameter; TIC, time-intensity curve; DCE-MRI, dynamic contrast-enhanced MRI; MRI, magnetic resonance imaging.

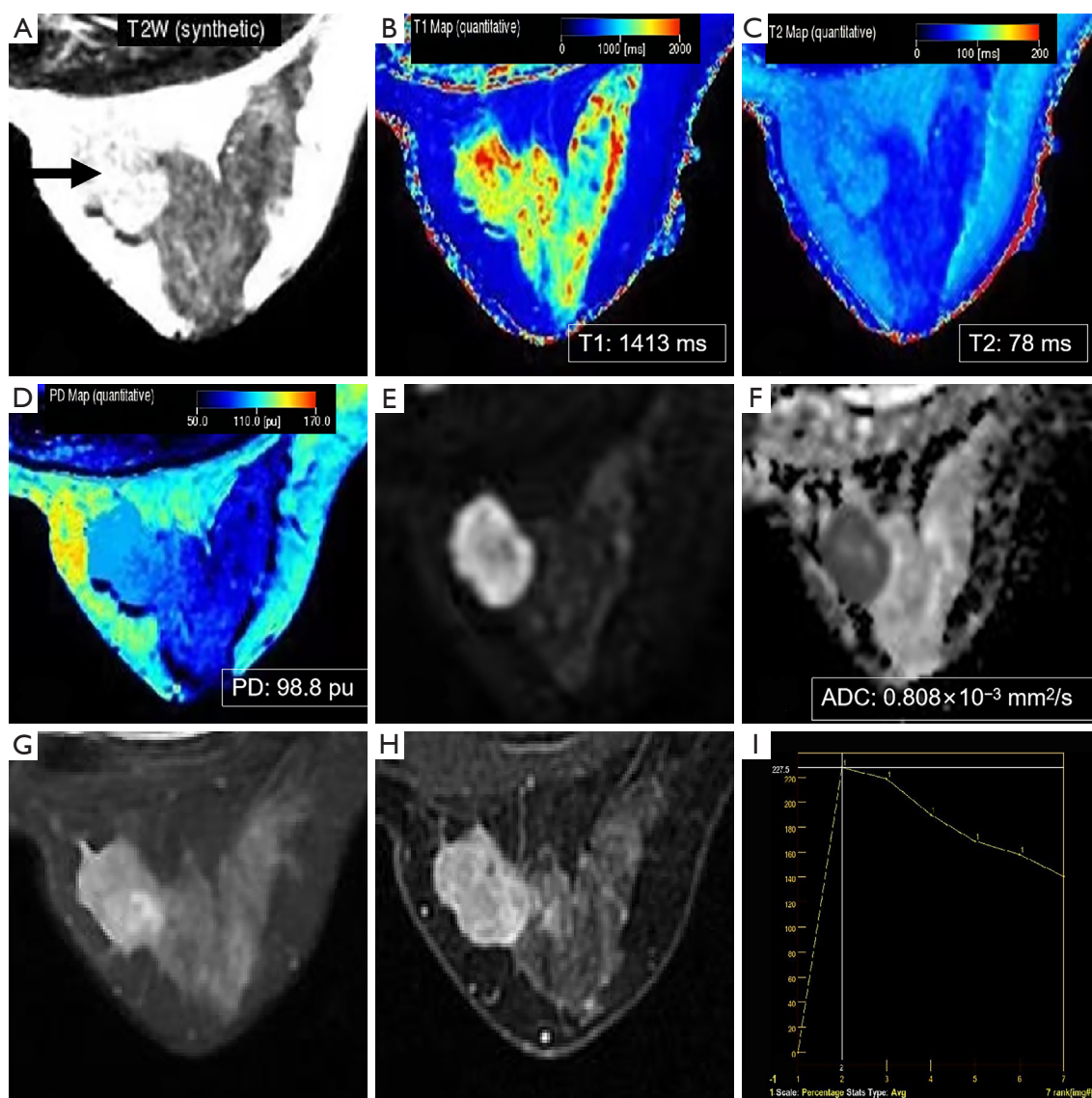


Figure 4 A 39-year-old female with breast cancer (arrow) and metastatic SLNs. (A) Synthetic T2-weighted image. (B-D) quantitative T1 map, T2 map, and PD map were acquired using syMRI; a T1 value of 1,413 ms, T2 value of 78 ms, and PD value of 98.8 pu are shown, respectively. (E) DWI ($b=1,000 \text{ s/mm}^2$), presenting homogenous hyperintensity in the tumor. (F) ADC map showing the ADC value of the tumor. (G) T2WI with fat saturation suppression showing a MaxAD of 2.9 cm, hyperintensity, and an irregular shape of the breast tumor. (H) Contrast-enhanced image showing internal homogeneous enhancement in the tumor. (I) TIC of DCE-MRI showing a washout enhancement type for the tumor. T2W, T2-weighted; T1, T1 relaxation time; T2, T2 relaxation time; PD, proton density; ADC, apparent diffusion coefficient; Avg, average; SLN, sentinel lymph node; syMRI, synthetic MRI; DWI, diffusion-weighted imaging; T2WI, T2-weighted imaging; MaxAD, maximum axis diameter; TIC, time-intensity curve; DCE-MRI, dynamic contrast-enhanced MRI; MRI, magnetic resonance imaging.

Table 3 Univariable and multivariable logistic regression analysis of factors related to metastatic SLNs of breast cancer

Factor	Univariable analysis			Multivariable analysis		
	β	OR (95% CI)	P value	β	OR (95% CI)	P value
Ki-67	1.35	3.859 (1.296–11.486)	0.01	0.774	2.169 (0.560–8.397)	0.26
Menopausal status	−0.824	0.438 (0.196–0.977)	0.04	−0.917	0.399 (0.138–1.151)	0.08
MaxAD	0.591	1.805 (1.111–2.932)	0.01	0.771	2.162 (1.116–4.189)	0.02
ADC	−3.921	0.019 (0.015–0.262)	0.003	−5.418	0.004 (0.002–0.089)	<0.001
PD	0.076	1.077 (1.034–1.123)	<0.001	0.126	1.134 (1.068–1.204)	<0.001

SLN, sentinel lymph node; β , regression coefficients; OR, odds ratio; CI, confidence interval; MaxAD, maximum axis diameter; ADC, apparent diffusion coefficient; PD, proton density.

Table 4 The performance of MRI features and parameters of breast tumors in predicting SLN metastases

Features and parameters	AUC (95% CI)	Cutoff value	Sensitivity (%)	Specificity (%)	PPV (%)	NPV (%)	Accuracy (%)	P value
syMRI								
PD (pu)	0.75 (0.659–0.835)	73.4	72.34	77.78	77.27	77.19	77.23	<0.001
DWI								
ADC ($\times 10^{-3}$ mm ² /s)	0.69 (0.593–0.780)	0.95	68.09	74.07	69.57	72.73	71.29	<0.001
Conventional MRI								
MaxAD (cm)	0.62 (0.519–0.716)	1.8	65.96	53.7	55.36	64.44	59.41	0.03
Combined model								
ADC + MaxAD	0.71 (0.618–0.802)	0.38	78.72	51.85	58.73	73.68	74.26	<0.001
PD + ADC + MaxAD	0.86 (0.778–0.922)	0.52	80.85	81.5	80.85	83.33	82.18	<0.001

MRI, magnetic resonance imaging; SLN, sentinel lymph node; AUC, area under the curve; CI, confidence interval; PPV, positive predictive value; NPV, negative predictive value; syMRI, synthetic MRI; PD, proton density; DWI, diffusion-weighted imaging; ADC, apparent diffusion coefficient; MaxAD, maximum axis diameter.

SLNs, providing additional value to the traditional MRI modalities. Moreover, we predicted the status of SLNs using noninvasive quantitative syMRI techniques, which provide valuable information about the tissue microenvironment. To the best of our knowledge, no study has used this technique for the prediction of SLN status. We obtained the quantitative PD value of the syMRI technique as an independent predictor through logistic regression analysis and constructed a joint prediction model by combining MaxAD and ADC, which yielded good predictive efficacy and resolved a clinical problem in patients with BC.

Previous studies have evaluated the characteristics of SLN or ALN status in BC using conventional MRI and radiomics features (12,26), diffusion imaging with different postprocessing models (10–12,27), and artificial neural networks (28). However, to the best of our knowledge,

few studies have reported on the clinical value of syMRI coupled with conventional and diffusion-weighted MRI in predicting SLNs metastases for patients with BC.

Moreover, SLNs, being typically closest to the breast tumor, are the station lymph nodes that are most likely to be metastasized by BC; therefore, they bear considerably more significance for clinical decision-making and treatment plans than do ALNs. However, SLNs themselves were often too small to be detected by MRI. Therefore, this study focused on the MRI features and quantitative parameters of the breast tumor to predict SLN metastases.

Within the scope of our investigation, we observed a substantial disparity in breast tumor size between lesions with metastatic SLNs and without metastatic SLNs, with the former demonstrating a remarkably larger size. Tumors' morphological features have been widely recognized as

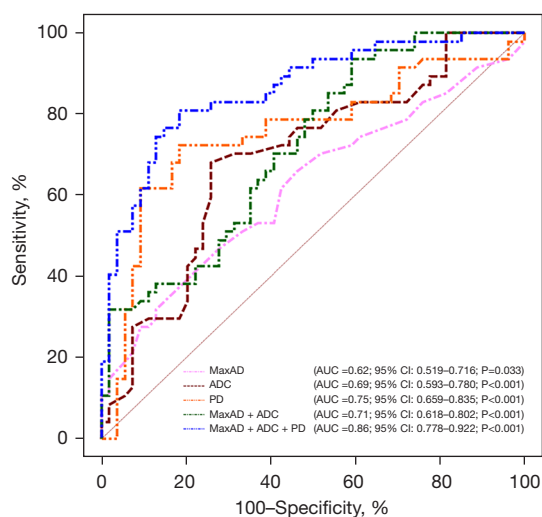


Figure 5 ROC curve analyses for MRI features and parameters of breast tumors were performed to predict metastatic SLNs in patients with breast cancer. MaxAD, maximum axis diameter; ADC, apparent diffusion coefficient; PD, proton density; AUC, area under the curve; CI, confidence interval; ROC, receiver operating characteristic; MRI, magnetic resonance imaging; SLN, sentinel lymph node.

essential factors associated with metastatic ALNs in BC (10,13). In our study, the size of the lesions with metastatic SLNs was significantly higher than that of those without metastatic SLNs, which was in line with earlier studies (12,29). The reason for this may be that the larger the size of the tumor is, the faster its growth and the more severe its malignancy. Therefore, larger-sized tumors may more likely to have SLN metastases.

This study showed that BCs with metastatic SLNs have lower ADC values compared to those without metastases. Previous studies have reported a significant correlation between lower tumor ADC and BC with metastatic SLNs (12,29), which is consistent with our findings. This may be attributed to the fact that DWI can provide quantitative information on water diffusion properties and the degree of diffusion restriction of water molecules in tissues. In aggressive tumors, increased cell density causes restricted water molecule movement and smaller extracellular space, leading to more restricted diffusion in malignant aggressive tumors. Therefore, DWI can be used as a noninvasive imaging method to determine if breast lesions have metastatic SLNs. Furthermore, in our study, the Ki-67 index was higher in SLNs-positive lesions than in the SLN-negative lesions. A high Ki-67 index may be associated with

more vigorous cell proliferation, which leads to higher cell density and lower ADC values (10,29,30).

We also found that the syMRI technique is helpful in identifying the metastatic SLN status of BCs. PD values in breast tumors with metastatic SLNs were confirmed to be significantly higher than those without metastatic SLNs. PD, derived from syMRI, as a magnetic property and quantitative parameter of tissue, essentially reflects the water content of tissue, making it a particularly sensitive metric in brain imaging for detecting edema and structural damage (31). One demonstrated the clinical utility of evaluating the status of lymph nodes in nasopharyngeal carcinoma by directly measuring PD values obtained from the lymph nodes (21). In the study conducted by Li *et al.*, it was found that breast IDC of higher histopathological grade exhibited statistically significant increases in PD values as compared to IDC of lower histopathological grades (32). Additionally, two studies provided evidence that IDC characterized by higher histopathological grades is associated with a higher incidence of lymph node metastasis, recurrence, and mortality (32,33). We speculate that BCs with metastatic SLNs seem to have a higher PD, resulting in a higher tissue water content and rendering them sensitive to structural damage and edema. Therefore, we believe that syMRI may have certain clinical value in identifying the status of SLNs in BC. Furthermore, syMRI and DWI are noninvasive imaging modalities that can be used for the preoperative evaluation of tumor characteristics. Consequently, quantitative tumor parameters could provide surgeons with information regarding SLN metastasis prior to surgery, aiding in the development of personalized treatment plans.

To improve the diagnostic efficiency, we first merged tumor MaxAD and ADC to construct a model for predicting metastatic SLNs in patients with BC, which resulted in a moderate diagnostic ability and an AUC of 0.71. We then added syMRI-derived PD to the model (MaxAD + ADC + PD), which yielded an increased AUC of 0.86, with a sensitivity of 80.85% and a specificity of 81.50%. In clinical practice, the use of this combined imaging method may be valuable for accurately predicting metastatic SLNs in those with BC. This finding may be particularly relevant for reducing unnecessary or inadequate ALN dissection during BC surgery. In addition to the morphological features of the tumors, syMRI provides useful information regarding the tissue microenvironment. Moreover, the combined model (AUC =0.86) can be used as a noninvasive method to improve the prediction performance of SLN

status in patients with BC, which can help clinicians make the appropriate surgical plan regarding whether to perform ALN dissection.

This study had some inherent limitations that should be mentioned. First, this study was conducted at a single center with a relatively small sample size. Hence, large-scale, multicenter research is needed to validate our findings. Second, all lesions had a MaxAD of more than 5 mm, and thus the characteristics of smaller lesions could have been overlooked and selection bias introduced. Third, our study was retrospective in nature, and a prospective study is needed to confirm the value of syMRI in determining the metastatic status of SLNs in BC. Fourth, this study included a small group of patients with noninvasive (n=11) or mucinous breast tumors (n=4), both of which have a lower rate of axially involvement than do invasive BCs. Finally, quantitative parameters measurements were performed on only one axial plane of the largest lesion diameter, which may not accurately capture the characteristics of the entire tumor.

Conclusions

A quantitative parameter (PD) from syMRI may be helpful in the prediction of SLN status in BC. The combination of PD, ADC, and MaxAD may serve as an effective strategy to improve the prediction of SLN metastases before surgery.

Acknowledgments

Funding: This study was funded by the Clinical Research and Translational Medicine Research Program of the Affiliated Hospital of Jiangnan University (contract No. YJY202305 to Z.S.).

Footnote

Reporting Checklist: The authors have completed the STARD reporting checklist. Available at <https://qims.amegroups.com/article/view/10.21037/qims-24-1/rc>

Conflicts of Interest: All authors have completed the ICMJE uniform disclosure form (available at <https://qims.amegroups.com/article/view/10.21037/qims-24-1/coif>). J.S. and W.D. are employees of GE HealthCare. The other authors have no conflicts of interest to declare.

Ethical Statement: The authors are accountable for all

aspects of the work in ensuring that questions related to the accuracy or integrity of any part of the work are appropriately investigated and resolved. The study was conducted according to the Declaration of Helsinki (as revised in 2013) and was approved by the Ethics Committee of Affiliated Hospital of Jiangnan University (No. LS2023090). Individual consent for this retrospective analysis was waived.

Open Access Statement: This is an Open Access article distributed in accordance with the Creative Commons Attribution-NonCommercial-NoDerivs 4.0 International License (CC BY-NC-ND 4.0), which permits the non-commercial replication and distribution of the article with the strict proviso that no changes or edits are made and the original work is properly cited (including links to both the formal publication through the relevant DOI and the license). See: <https://creativecommons.org/licenses/by-nc-nd/4.0/>.

References

1. Sung H, Ferlay J, Siegel RL, Laversanne M, Soerjomataram I, Jemal A, Bray F. Global Cancer Statistics 2020: GLOBOCAN Estimates of Incidence and Mortality Worldwide for 36 Cancers in 185 Countries. *CA Cancer J Clin* 2021;71:209-49.
2. Amlicke MJ, Park J, Agala CB, Casey DL, Ray EM, Downs-Canner SM, Spanheimer PM. Prevalence of Pathologic N2/N3 Disease in Postmenopausal Women with Clinical N0 ER+/HER2- Breast Cancer. *Ann Surg Oncol* 2022;29:7662-9.
3. Morrow M. Is Axillary Staging Obsolete in Early Breast Cancer? *Surg Oncol Clin N Am* 2023;32:675-91.
4. Zhang-Yin J, Mael E, Talpe S. Update on Sentinel Lymph Node Methods and Pathology in Breast Cancer. *Diagnostics (Basel)* 2024;14:252.
5. Zheng Y, Sun J, Zhu L, Hu MS, Hou LZ, Liu JX, Dong FL. Diagnosing sentinel lymph node metastasis of T1/T2 breast cancer with conventional ultrasound combined with double contrast-enhanced ultrasound: a preliminary study. *Quant Imaging Med Surg* 2023;13:3451-63.
6. Zhu Y, Jia Y, Pang W, Duan Y, Chen K, Nie F. Ultrasound contrast-enhanced patterns of sentinel lymph nodes: predictive value for nodal status and metastatic burden in early breast cancer. *Quant Imaging Med Surg* 2023;13:160-70.
7. Tinterri C, Canavese G, Gatzemeier W, Barbieri E, Bottini A, Sagona A, Caraceni G, Testori A, Di Maria Grimaldi

- S, Dani C, Boni L, Bruzzi P, Fernandes B, Scorsetti M, Zambelli A, Gentile D; SINODAR-ONE Collaborative Group. Sentinel lymph node biopsy versus axillary lymph node dissection in breast cancer patients undergoing mastectomy with one to two metastatic sentinel lymph nodes: sub-analysis of the SINODAR-ONE multicentre randomized clinical trial and reopening of enrolment. *Br J Surg* 2023;110:1143-52.
8. Wu SY, Li JW, Wang YJ, Jin KR, Yang BL, Li JJ, Yu XL, Mo M, Hu N, Shao ZM, Liu GY. Clinical feasibility and oncological safety of non-radioactive targeted axillary dissection after neoadjuvant chemotherapy in biopsy-proven node-positive breast cancer: a prospective diagnostic and prognostic study. *Int J Surg* 2023;109:1863-70.
 9. Barrio AV, Montagna G, Mamtani A, Sevilimedu V, Edelweiss M, Capko D, Cody HS 3rd, El-Tamer M, Gemignani ML, Heerdt A, Kirstein L, Moo TA, Pilewskie M, Plitas G, Sacchini V, Sclafani L, Tadros A, Van Zee KJ, Morrow M. Nodal Recurrence in Patients With Node-Positive Breast Cancer Treated With Sentinel Node Biopsy Alone After Neoadjuvant Chemotherapy-A Rare Event. *JAMA Oncol* 2021;7:1851-5.
 10. Zhao M, Wu Q, Guo L, Zhou L, Fu K. Magnetic resonance imaging features for predicting axillary lymph node metastasis in patients with breast cancer. *Eur J Radiol* 2020;129:109093.
 11. Razek AA, Lattif MA, Denewer A, Farouk O, Nada N. Assessment of axillary lymph nodes in patients with breast cancer with diffusion-weighted MR imaging in combination with routine and dynamic contrast MR imaging. *Breast Cancer* 2016;23:525-32.
 12. Choi EJ, Youk JH, Choi H, Song JS. Dynamic contrast-enhanced and diffusion-weighted MRI of invasive breast cancer for the prediction of sentinel lymph node status. *J Magn Reson Imaging* 2020;51:615-26.
 13. Kim JY, Seo HB, Park S, Moon JI, Lee JW, Lee NK, Lee SW, Bae YT. Early-stage invasive ductal carcinoma: Association of tumor apparent diffusion coefficient values with axillary lymph node metastasis. *Eur J Radiol* 2015;84:2137-43.
 14. Warntjes JB, Leinhard OD, West J, Lundberg P. Rapid magnetic resonance quantification on the brain: Optimization for clinical usage. *Magn Reson Med* 2008;60:320-9.
 15. Warntjes JB, Dahlqvist O, Lundberg P. Novel method for rapid, simultaneous T1, T2*, and proton density quantification. *Magn Reson Med* 2007;57:528-37.
 16. Jung Y, Gho SM, Back SN, Ha T, Kang DK, Kim TH. The feasibility of synthetic MRI in breast cancer patients: comparison of T(2) relaxation time with multiecho spin echo T(2) mapping method. *Br J Radiol* 2019;92:20180479.
 17. Cui Y, Han S, Liu M, Wu PY, Zhang W, Zhang J, Li C, Chen M. Diagnosis and Grading of Prostate Cancer by Relaxation Maps From Synthetic MRI. *J Magn Reson Imaging* 2020;52:552-64.
 18. Gao W, Zhang S, Guo J, Wei X, Li X, Diao Y, Huang W, Yao Y, Shang A, Zhang Y, Yang Q, Chen X. Investigation of Synthetic Relaxometry and Diffusion Measures in the Differentiation of Benign and Malignant Breast Lesions as Compared to BI-RADS. *J Magn Reson Imaging* 2021;53:1118-27.
 19. Cai Q, Wen Z, Huang Y, Li M, Ouyang L, Ling J, Qian L, Guo Y, Wang H. Investigation of Synthetic Magnetic Resonance Imaging Applied in the Evaluation of the Tumor Grade of Bladder Cancer. *J Magn Reson Imaging* 2021;54:1989-97.
 20. Ge YX, Hu SD, Wang Z, Guan RP, Zhou XY, Gao QZ, Yan G. Feasibility and reproducibility of T2 mapping and DWI for identifying malignant lymph nodes in rectal cancer. *Eur Radiol* 2021;31:3347-54.
 21. Wang P, Hu S, Wang X, Ge Y, Zhao J, Qiao H, Chang J, Dou W, Zhang H. Synthetic MRI in differentiating benign from metastatic retropharyngeal lymph node: combination with diffusion-weighted imaging. *Eur Radiol* 2022;33:152-61.
 22. D'Orsi CJ, Sickles EA, Mendelson EB, Morris EA. ACR BI-RADS Atlas: Breast Imaging Reporting and Data System, 5th ed. American College of Radiology, 2013.
 23. Sogani J, Morris EA, Kaplan JB, D'Alessio D, Goldman D, Moskowitz CS, Jochelson MS. Comparison of Background Parenchymal Enhancement at Contrast-enhanced Spectral Mammography and Breast MR Imaging. *Radiology* 2017;282:63-73.
 24. Cheang MC, Chia SK, Voduc D, Gao D, Leung S, Snider J, Watson M, Davies S, Bernard PS, Parker JS, Perou CM, Ellis MJ, Nielsen TO. Ki67 index, HER2 status, and prognosis of patients with luminal B breast cancer. *J Natl Cancer Inst* 2009;101:736-50.
 25. Elston CW, Ellis IO. Pathological prognostic factors in breast cancer. I. The value of histological grade in breast cancer: experience from a large study with long-term follow-up. *Histopathology* 1991;19:403-10.
 26. Cui X, Wang N, Zhao Y, Chen S, Li S, Xu M, Chai R. Preoperative Prediction of Axillary Lymph Node

- Metastasis in Breast Cancer using Radiomics Features of DCE-MRI. *Sci Rep* 2019;9:2240.
27. Kurt N, Binboga Kurt B, Gulsaran U, Uslu B, Celik AO, Sut N, Tastekin E, Karabulut D, Tuncbilek N. Diffusion tensor imaging and diffusion-weighted imaging on axillary lymph node status in breast cancer patients. *Diagn Interv Radiol* 2022;28:329-36.
 28. Dietzel M, Baltzer PA, Dietzel A, Vag T, Gröschel T, Gajda M, Camara O, Kaiser WA. Application of artificial neural networks for the prediction of lymph node metastases to the ipsilateral axilla - initial experience in 194 patients using magnetic resonance mammography. *Acta Radiol* 2010;51:851-8.
 29. Dong Y, Feng Q, Yang W, Lu Z, Deng C, Zhang L, Lian Z, Liu J, Luo X, Pei S, Mo X, Huang W, Liang C, Zhang B, Zhang S. Preoperative prediction of sentinel lymph node metastasis in breast cancer based on radiomics of T2-weighted fat-suppression and diffusion-weighted MRI. *Eur Radiol* 2018;28:582-91.
 30. Ozemir IA, Orhun K, Eren T, Baysal H, Sagioglu J, Leblebici M, Ceyran AB, Alimoglu O. Factors affecting sentinel lymph node metastasis in Turkish breast cancer patients: Predictive value of Ki-67 and the size of lymph node. *Bratisl Lek Listy* 2016;117:436-41.
 31. Gracien RM, Reitz SC, Hof SM, Fleischer V, Zimmermann H, Droby A, Steinmetz H, Zipp F, Deichmann R, Klein JC. Changes and variability of proton density and T1 relaxation times in early multiple sclerosis: MRI markers of neuronal damage in the cerebral cortex. *Eur Radiol* 2016;26:2578-86.
 32. Li Q, Xiao Q, Yang M, Chai Q, Huang Y, Wu PY, Niu Q, Gu Y. Histogram analysis of quantitative parameters from synthetic MRI: Correlations with prognostic factors and molecular subtypes in invasive ductal breast cancer. *Eur J Radiol* 2021;139:109697.
 33. Bansal C, Pujani M, Sharma KL, Srivastava AN, Singh US. Grading systems in the cytological diagnosis of breast cancer: a review. *J Cancer Res Ther* 2014;10:839-45.

Cite this article as: Yang X, Lu Z, Tan X, Shao L, Shi J, Dou W, Sun Z. Evaluating the added value of synthetic magnetic resonance imaging in predicting sentinel lymph node status in breast cancer. *Quant Imaging Med Surg* 2024;14(6):3789-3802. doi: 10.21037/qims-24-1